Observation of Magnetic Ripple and Nanowidth Domains in a Layered Ferromagnet

T. Asaka,[1] T. Kimura,[2] T. Nagai,[1] X. Z. Yu,[1,3] K. Kimoto,[1] Y. Tokura,[3,4,5] and Y. Matsui[1]

[1]*High Voltage Electron Microscopy Station (HVEMS), National Institute for Materials Science (NIMS), Tsukuba 305-0044, Japan*
[2]*Los Alamos National Laboratory, Los Alamos, New Mexico 87545, USA*
[3]*Spin Superstructure Project, Exploratory Research for Advanced Technology (ERATO), Japan Science and Technology Agency (JST), Tsukuba 305-8562, Japan*
[4]*Department of Applied Physics, University of Tokyo, Tokyo 113-8656, Japan*
[5]*Correlated Electron Research Center (CERC), National Institute of Advanced Industrial Science and Technology (AIST), Tsukuba 305-0046, Japan*

(Received 4 July 2005; published 22 November 2005)

We investigated ferromagnetic domain structures on nanometer to micrometer scale for single crystals of a layered ferromagnet, $La_{2-2x}Sr_{1+2x}Mn_2O_7$ ($0.32 \leq x \leq 0.40$), as functions of x and temperature by means of Lorentz electron microscopy. We have succeeded in observing the evolution of magnetic ripple structure, dynamically, related to a spin reorientation transition where the magnetization direction switches between parallel and perpendicular to the layers. Our high-resolution magnetic domain imaging revealed that the ripple state is characterized by the evolution of magnetic nanowidth domains.

DOI: 10.1103/PhysRevLett.95.227204 PACS numbers: 75.60.Ch, 75.25.+z, 75.30.Gw, 75.30.Kz

Magnetic domain structure in a ferromagnet is a natural consequence of the various contributions to the total free energy such as magnetostatic, exchange, anisotropy, and magnetoelastic interactions [1,2]. In ferromagnets with strongly correlated electrons, these interactions are very sensitive to a small perturbation, such as a change in temperature, magnetic field, pressure, and chemical composition [3]. Therefore, it is likely that a wide variety of magnetic domain structures is realized and tunable in these systems.

A layered magnetic system, $La_{2-2x}Sr_{1+2x}Mn_2O_7$, has been investigated extensively in the past decade because of intriguing magnetic-field-induced phenomena such as colossal magnetoresitive [4], tunneling-type magnetoresistive [5], and giant magnetostrictive effects [6]. $La_{2-2x}Sr_{1+2x}Mn_2O_7$, having the $I4/mmm$ tetragonal structure, is composed of ferromagnetic (FM) MnO_2 bilayers with intervening insulating $(La, Sr)_2O_2$ blocks, as illustrated in Fig. 1. One of the most characteristic features in the layered system is that a variety of antiferromagnetic and FM ground states turn up as a function of the doping level x owing to critical x dependence of the exchange interactions of intra- and interbilayers (Fig. 1) [7–10]. At $0.32 \lesssim x \lesssim 0.42$, $La_{2-2x}Sr_{1+2x}Mn_2O_7$ exhibits the FM ground states with the Curie temperatures $T_C =$ 100–130 K. There exist two kinds of FM ground states. The magnetic moments are polarized along the tetragonal c axis for $x \lesssim 0.33$, whereas those for $x \gtrsim 0.33$ lie within the ab plane. Namely, doping-induced spin reorientation transition (SRT) occurs at around $x \sim 0.33$ in the layered ferromagnet. The evolution of the magnetic structures has been discussed in terms of the change of the relative occupancy in two e_g-type orbitals ($3z^2 - r^2$ and $x^2 - y^2$) [7–12].

It is expected that the SRT of the layered manganite affects the magnetic domain structure. In order to image the magnetic domain structures of $La_{2-2x}Sr_{1+2x}Mn_2O_7$ ($0.32 \leq x \leq 0.40$), we used Lorentz transmission electron microscopy (LTEM). Several research groups have reported the magnetic domain structures in $La_{2-2x}Sr_{1+2x}Mn_2O_7$ single crystals by means of a scanning Hall probe [13] and a magneto-optical technique [14,15]. However, the spatial resolution of these techniques is only down to micrometer scale. LTEM is characterized by high resolution on the nanometer scale and high sensitivity to small variations in magnetization. Furthermore, we can observe the interaction between domain walls and lattice defects directly and dynamic behavior of domains in real time. In addition, LTEM enables us to observe images of

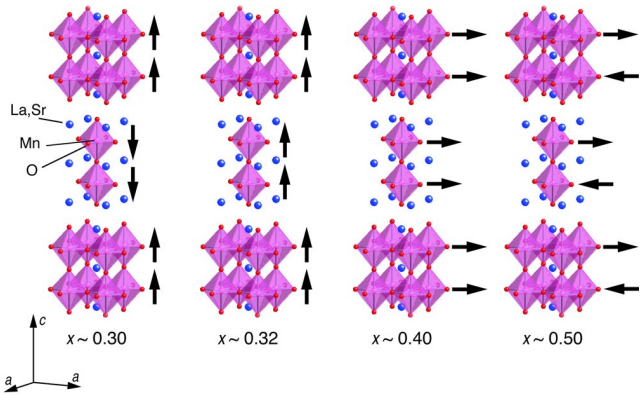

FIG. 1 (color online). Evolution of the ground-state magnetic structures in $La_{2-2x}Sr_{1+2x}Mn_2O_7$ ($0.30 \leq x \leq 0.50$) [extracted from Refs. [7,9]]. Arrows on the right of the respective crystal structures represent the magnetic moment of Mn within a single MnO_2 layer unit.

not only the cleaved *ab* face but also the *ac* face, which is of great advantage over spin-polarized scanning electron microscopy [16]. Besides, the phase separation has been observed between the ferromagnetic phase and the antiferromangetic charge-ordered one in manganites on nanometer to micrometer scale by the LTEM technique [17–19].

Single crystals of $La_{2-2x}Sr_{1+2x}Mn_2O_7$ ($x = 0.32$–0.40) were grown by a floating-zone method, as described in detail elsewhere [20]. For the observation using Lorentz electron microscope, the crystals were oriented using Laue x-ray diffraction patterns, cut into thin plates, and thinned by a mechanical grinding and an Ar^+ ion sputtering. The specimens were cooled at temperatures between room temperature and 17 K and were examined using a field-emission gun Lorentz electron microscope (Hitachi HF-3000L) operating at 300 kV. The microscope is equipped with a custom-made objective lens, which makes magnetic fields at sample position almost zero. The specimen thickness in the observed area was ~150 nm or less. Fresnel and Foucault methods were used for LTEM observation. The principles of imaging in the Fresnel and the Foucault methods of LTEM have been given elsewhere [21,22]. No magnetic field was applied throughout this work.

We display in Fig. 2 the variation of magnetic domain structures depending on x. Upper and lower panels show images of thin plates parallel to the *ab* and *ac* planes, respectively. These electron micrographs were taken at 17 K with the Fresnel mode in the LTEM. In the Fresnel images, the characteristic black and white lines, which exhibit an alternating array in most cases, correspond to domain walls. The broad curved black lines are bend contours. The insets of the respective Fresnel images show direct beam images under the diffraction mode. The direct beam images display results of the deflection of the electron beam by the Lorentz force which is caused by magnetization in the specimen. Therefore, the magnetic domains have the magnetization perpendicular to the direction of the deflection of electron beam. For the $x = 0.32$ specimen, we observed dense stripe domains with the width of about 120 nm in the image of the *ab* thin plate [Fig. 2(a)] and wide 180° domains extended to the *c* axis in the image of the *ac* thin plate [Fig. 2(e)]. Generally, the stripe-domain structure is characteristic of ferromagnetic materials with the uniaxial magnetic anisotropy perpendicular to the thin film [23]. Such a stripe-domain structure has a periodic wavy structure in the magnetization direction, which is caused by the competition between the magnetostatic and the magnetocrystalline anisotoropic energies. However, according to our LTEM observation, the observed stripe-domain structure exhibits a narrow proper 180° domain structure, though there are significant out-of-plane magnetic components at the domain walls, i.e., wide Bloch-type domain wall structure. On the contrary, wide in-plate 180° domain structures, extended in the directions of [100] and [110], were observed in the $x = 0.36$ and 0.40 specimens, where the easy axis of magnetization lies within the *ab* plane [Figs. 2(c), 2(d), 2(g), and 2(h)]. In the intermediate $x = 0.33$ specimen, which is located on the verge of the SRT, coexistence of the uniaxial (the *c* axis) and the in-plane anisotropic domains was revealed as shown in Figs. 2(b) and 2(f). The coexistence resulted in a combination of both the dense stripe domains and the ordinary 180° domains in the *ab* thin plate and the formation of the 90° domain structure in the *ac* thin plate. Our observation clearly demonstrates that the magnetic domain structures in $La_{2-2x}Sr_{1+2x}Mn_2O_7$ vary significantly with the doping level x. This may be closely related to the above-mentioned strong x dependence of the magnetic anisotropy and be a rare phenomenon that the magnetic domain structures drastically vary with slight change in the chemical composition.

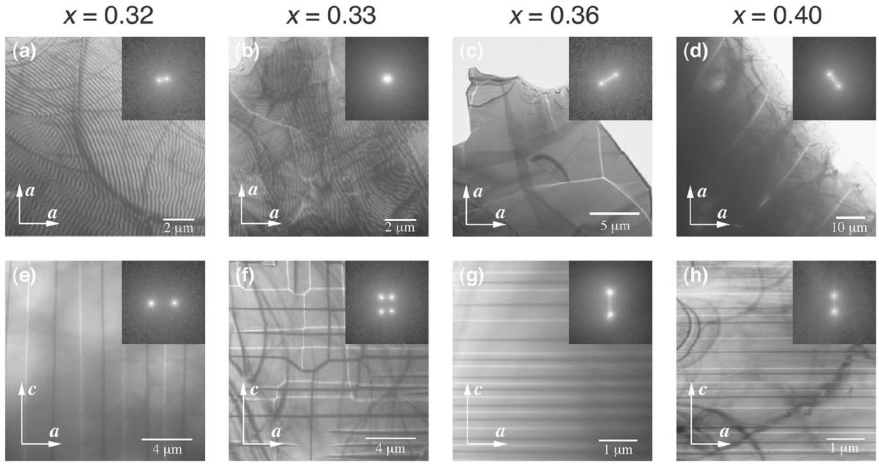

FIG. 2. Doping-level dependence of magnetic domain structures at low temperatures (~17 K) in $La_{2-2x}Sr_{1+2x}Mn_2O_7$. (a)–(d) [001]-zone and (e)–(h) [010]-zone Fresnel images for the $x = 0.32$ [(a) and (e)], 0.33 [(b) and (f)], 0.36 [(c) and (g)], and 0.4 [(d) and (h)] specimens. The insets of the respective Fresnel images are the corresponding direct beam images under the diffraction mode. The relatively sharp black and white lines in each Fresnel image represent images of domain walls.

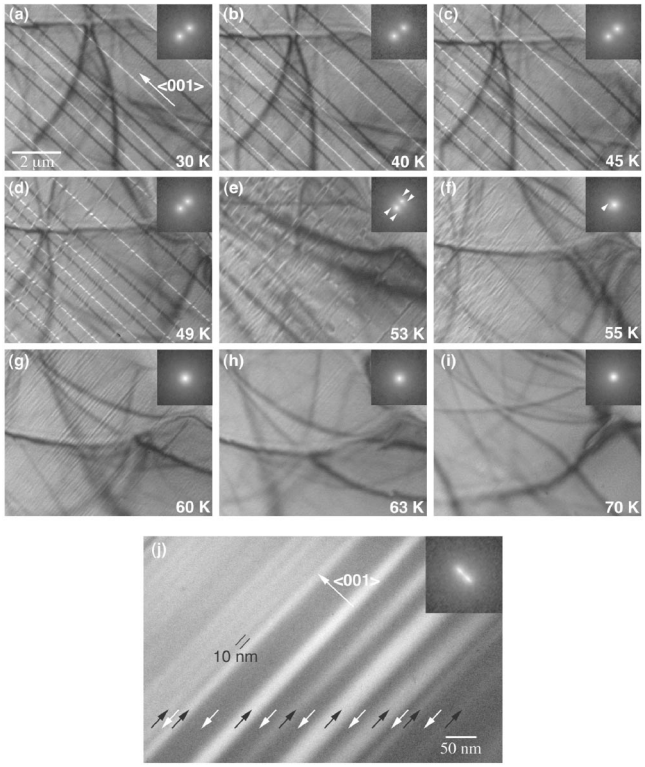

FIG. 3. Temperature profiles of magnetic domain structures for $La_{2-2x}Sr_{1+2x}Mn_2O_7$ ($x = 0.32$). The LTEM images of (a)–(i) were taken with Fresnel mode. The insets of the respective Fresnel images are the corresponding direct beam images under the diffraction mode. These images were taken for the *ac* plane. In Fresnel images, ripple contrasts appeared perpendicular to the *c* axis for 50–70 K. In the direct beam image, white arrowheads indicate very weak streaks. (j) A Foucalt image of ripple contrast at 60 K. Arrows indicate the directions of magnetization at the respective domains. The inset in (j) shows the corresponding direct beam image focused on the ripple contrast.

For $x = 0.30$ and 0.32, as increasing temperature, the SRTs from the *c* axis towards the *ab* plane were reported [14,16,24,25]. We show in Fig. 3 the dynamic behavior of the magnetic domain structures for the *ac* thin plate of the $x = 0.32$ specimen. The magnetic ripple state was observed at 50–70 K around the SRT temperature. On heating from 30 K, we could observe ordinary 180° domains extended along the *c* axis up to ~50 K. When the temperature increased above 50 K, some streaks appeared perpendicular to the domain walls, accompanying a cross-tie-wall image around crossover of the 180° domain walls. These streaks developed with increasing temperature. Upon further heating, ordinary 180° domain walls gradually disappeared above ~55 K, and only the streaks remained. Here the remaining streaks look like ripple contrast. The ripple contrast was gradually reduced above 65 K and vanished at ~70 K. We also observed the ripple contrast in the cooling process. The behavior of the magnetic domain structures in the cooling process was similar to that in the heating process. Usually, the ripple contrast is observed in polycrystalline magnetic thin films, indicating the fluctuation of local magnetization by the crystal anisotropy of individual grains [26,27]. Accordingly, the ordinary ripple contrast does not have an orientation. To realize a linear ripple state as observed in this study, a post-treatment such as a magnetic annealing [28] and/or a fabrication of a multilayer thin film [29,30] would have to be required for other materials. Note that the observed ripple state appeared spontaneously in the single-crystalline sample with no artificial nanotexture.

The temperature profiles of the direct beam shown in the insets in Fig. 3 correspond to the behavior of the domain structures observed in the Fresnel images. Direct beams were obviously split into two spots at temperatures below 53 K. This split is caused by Lorentz force in the 180° domain structure. Around 53 K, we observed very weak streaks through the direct beams along the *c* axis (indicated by white arrows in the inset in Fig. 3). This suggests local variation of magnetic induction that deviates from the matrix spin direction and that the magnetic components with the direction of magnetization perpendicular to the *c* axis exist. The streaks should correspond to the ripple contrasts in the Fresnel images. The split two direct beams united into one, because the ordinary 180° domain disappeared at temperatures above 55 K.

To scrutinize more details of the ripple contrast, we carried out the Foucault imaging in the LTEM. Here, in a Foucault image, both black and white regions indicate the magnetic domains. Figure 3(j) is a Foucault image of the ripple contrast in the Fresnel image [Fig. 3(g)] at 60 K. The inset in Fig. 3(j) shows the corresponding direct beam image, which was focused on the ripple contrast. According to Fig. 3(j), the observed magnetic state exhibits a narrow 180° domain structure with the magnetization di-

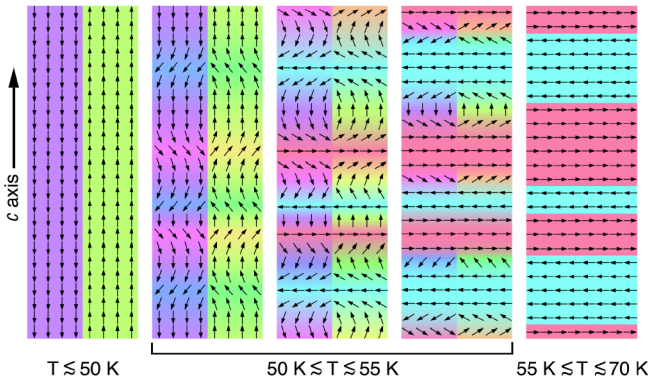

FIG. 4 (color online). Proposed model of the evolution of a magnetic ripple state in $La_{2-2x}Sr_{1+2x}Mn_2O_7$ ($x = 0.32$). Arrows represent the local magnetic moment. Below 50 K, the magnetic domains exhibit ordinary 180° domain structure. The two phases with the easy axis either parallel or perpendicular to the *c* axis coexist at temperatures of ~50–55 K. Above ~55 K, the magnetization direction becomes completely along the *ab* plane, and the ripple state that consists of platelike magnetic nanowidth domains evolves at temperatures of ~55–70 K.

rection perpendicular to the c axis. Width of each domain is from ~10 to ~50 nm. Therefore, we conclude that the ripple contrast in the Fresnel images signifies the presence of platelike magnetic nanowidth domains with the magnetization direction along the ab plane.

In Fig. 4, we illustrate the process of formation of the ripple state, i.e., nanowidth domains. Arrows in Fig. 4 indicate the local magnetic moments. Below 50 K, the magnetic domains exhibit ordinary 180° domain structure. Above 50 K, narrow parts with the fluctuations of the magnetic moments grow like planar faults. With increasing temperature, the fluctuation parts develop, and the platelike magnetic nanowidth domains are formed with the direction of magnetization perpendicular to the c axis. The two phases with the easy axis either parallel or perpendicular to the c axis coexist at temperatures of 50–55 K. Above 55 K, the magnetization direction becomes completely perpendicular to the c axis, i.e., along the ab plane, and the ripple state that consists of platelike magnetic nanowidth domains evolves at temperatures of 55–70 K. We conclude that the ripple state is related to the two-dimensional fluctuation of magnetic moments and the evolution of the platelike magnetic nanowidth domains around the SRT temperature.

Finally, we discuss the origin of the ripple state and the temperature-induced SRT in $La_{2-2x}Sr_{1+2x}Mn_2O_7$ ($x = 0.32$). The evolution of the ripple state can be regarded as the two-dimensional spread of magnetic domain and suppression of growth to the direction along the c axis. In addition, the ripple state evolved linearly perpendicular to the c axis. Therefore, the mode of formation of the ripple state is undoubtedly caused by the two-dimensional crystal structure, and the MnO_6-bilayer obviously plays a role as a unit of the platelike magnetic nanowidth domain. Concerning the doping dependence of e_g-orbital states on Mn sites, the e_g electrons in the MnO_6 bilayers prefer to occupy mainly $d_{3z^2-r^2}$ orbital at low doping and mostly $d_{x^2-y^2}$ at high doping [6–11]. Furthermore, the doping-induced uniaxial-to-in-plane SRT seems to occur concomitantly with the orbital-state transition. We consider that, as in this case, the temperature-induced SRT is also caused by the $d_{3z^2-r^2}$-to-$d_{x^2-y^2}$ orbital-state transition. Concerning the temperature dependence of orbital states in $La_{2-2x}Sr_{1+2x}Mn_2O_7$, Kimura *et al.* demonstrated that, in the temperature dependence of the elastic property, an anomaly of the striction along the ab plane in the $x = 0.32$ specimen was observed at around 60 K [6]. This would provide collateral evidence for the proposal that the $d_{3z^2-r^2}$-to-$d_{x^2-y^2}$ orbital-state transition occurs around 50–55 K. Moreover, since such orbital states can evolve two-dimensionally due to the layered structure, the magnetic domains may become a platelike shape with nanowidth along the ab plane. The observation suggests that the control of orbital state provides a new SRT phenomenon with the appearance of the nanowidth domain.

In this study, we have observed the evolution of magnetic domain structures in single crystals of $La_{2-2x}Sr_{1+2x}Mn_2O_7$ ($0.32 \leq x \leq 0.40$) and found a magnetic ripple state, which signifies a formation of magnetic nanodomain at spin reorientation transition temperature. The results provide not only a variety of magnetic domain structures in ferromagnetic systems with correlated electrons but also a new possibility for memory devices with ultrahigh density.

We thank C. Tsuruta for help with the TEM experiments, and S. Mori, T. Arima, M. Konoto, Y. Horibe, and Y. Kaneko for fruitful discussions. A part of this work was supported by ''Nanotechnology Support Project'' of the Ministry of Education, Culture, Sports, Science and Technology (MEXT), Japan.

[1] A. Hubert and R. Schäfer, *Magnetic Domains: The Analysis of Magnetic Microstructures* (Springer-Verlag, Berlin, 1998).
[2] S. Chikazumi, *Physics of Ferromagnetism* (Oxford University, New York, 1997).
[3] M. Imada, A. Fujimori, and Y. Tokura, Rev. Mod. Phys. **70**, 1039 (1998).
[4] Y. Moritomo *et al.*, Nature (London) **380**, 141 (1996).
[5] T. Kimura *et al.*, Science **274**, 1698 (1996).
[6] T. Kimura *et al.*, Phys. Rev. Lett. **81**, 5920 (1998).
[7] T. Kimura and Y. Tokura, Annu. Rev. Mater. Sci. **30**, 451 (2000).
[8] M. Kubota *et al.*, J. Phys. Soc. Jpn. **69**, 1606 (2000).
[9] J. F. Mitchell *et al.*, J. Phys. Chem. B **105**, 10 731 (2001).
[10] K. Hirota *et al.*, Phys. Rev. B **65**, 064414 (2002).
[11] A. Koizumi *et al.*, Phys. Rev. Lett. **86**, 5589 (2001).
[12] G. Jackeli and N. B. Perkins, Phys. Rev. B **65**, 212402 (2002).
[13] T. Fukumura *et al.*, Science **284**, 1969 (1999).
[14] U. Welp *et al.*, Phys. Rev. B **62**, 8615 (2000).
[15] Y. Tokunaga, M. Tokunaga, and T. Tamegai, Phys. Rev. B **71**, 012408 (2005).
[16] M. Konoto *et al.*, Phys. Rev. Lett. **93**, 107201 (2004).
[17] S. Mori, T. Asaka, and Y. Matsui, J. Electron Microsc. **51**, 225 (2002).
[18] J. C. Loudon, N. D. Mathur, and P. A. Midgley, Nature (London) **420**, 797 (2002).
[19] S. Mori *et al.*, Phys. Rev. B **67**, 012403 (2003).
[20] T. Kimura *et al.*, Phys. Rev. B **58**, 11 081 (1998).
[21] P. J. Grundy and R. S. Tebble, Adv. Phys. **17**, 153 (1968).
[22] P. B. Hirsch *et al.*, *Electron Microscopy of Thin Crystals* (Krieger, Malabar, FL, 1977).
[23] N. Saito, H. Fujiwara, and Y. Sugita, J. Phys. Soc. Jpn. **19**, 421 (1964).
[24] T. G. Perring *et al.*, Phys. Rev. B **58**, R14 693 (1998).
[25] D. N. Argyriou *et al.*, Phys. Rev. B **59**, 8695 (1999).
[26] H. Hoffmann, IEEE Trans. Magn. **4**, 32 (1968).
[27] K. J. Harte, J. Appl. Phys. **39**, 1503 (1968).
[28] M. S. Cohen, J. Appl. Phys. **34**, 1841 (1963).
[29] X. Portier and A. K. Petford-Long, J. Phys. D: Appl. Phys. **32**, R89 (1999).
[30] C. L. Platt *et al.*, Phys. Rev. B **61**, 9633 (2000).